Hirdaris, Spyros; Zhang, Mingyang; Tsoulakos, Nikolaos; Kujala, Pentti

A Ship Digital Twin for Safe and Sustainable Ship Operations

Published in:
State-of-the-Art Digital Twin Applications for Shipping Sector Decarbonization

DOI:
10.4018/978-1-6684-9848-4.ch009

Published: 01/01/2024

Document Version
Publisher's PDF, also known as Version of record

Chapter 9
A Ship Digital Twin for Safe and Sustainable Ship Operations

Spyros Hirdaris
https://orcid.org/0000-0002-4700-6325
American Bureau of Shipping, Greece

Mingyang Zhang
https://orcid.org/0000-0001-5820-2789
Aalto University, Finland

Nikos Tsoulakos
Laskaridis Shipping Co. Ltd., Greece

Pentti Kujala
Taltech, Estonia

ABSTRACT

Shipping is responsible for over 90% of global trade. Although it is generally considered a safe and clean mode of transportation, it still has a significant impact on the environment. Thus, state-of-the-art models that may contribute to the sustainable management of the life cycle of shipping operations without compromising safety standards are urgently needed. This chapter discusses the potential of artificial intelligence (AI) based digital twin models to monitor ship safety and efficiency. A paradigm shift is introduced in the form of a model that can predict ship motions and fuel consumption under real operational conditions using deep learning models. A bi-directional long short-term memory (LSTM) network with attention mechanisms is used to predict ship fuel consumption and a transformer neural network is employed to capture ship motions in realistic hydrometeorological conditions. By comparing the predicted results with available full scale measurement data, it is suggested that following further testing and validation, these models could perform satisfactorily in real conditions. Accordingly, they could be integrated into a framework for safe and sustainable ship operations.

DOI: 10.4018/978-1-6684-9848-4.ch009

INTRODUCTION

Shipping plays a crucial role in global trade, accounting for over 90% of the transportation of goods worldwide (UNCTAD, 2022). While it is generally considered a safe and environmentally friendly mode of transport, it still has a significant impact on the environment (UNFCCC, 2022). As a result, there is a growing need to ensure the safety and sustainability of ship operations by embracing modern technology.

Originally developed by NASA, digital twins involve creating a virtual replica of a physical object or system to simulate and analyse its performance in real-time (Allen, 2021; Zhang, Hirdaris, & Tsoulakos, 2023). They can be described as machines or computer-based models that simulate, emulate, mirror, or "twin" the existence of a physical entity. For example, a ship digital twin refers to a virtual replica or representation of a real ship. This digital replica can be created by combining real-time data, simulation models, and advanced analytics, allowing for visualization, analysis, and optimization that aims to assure safe and sustainable operations in real operations (see Figure 1).

It is important to acknowledge that the accuracy of physics-based models may be limited to "as build" design or when it comes to dealing with complex operational conditions and extreme events (Kaur et al., 2020). Through deep learning algorithms offer the potential to improve the predictive capabilities of digital twin models (Huang et al., 2021; Lee et al., 2022; Nielsen et al., 2022). To address the challenges associated with predictive analytics and visualisation hybrid methods should be employed. For example, digital twin optimal deep learning models are designed to accurately predict ship motions (Nielsen et al., 2022; Zhang, Taimuri, Zhang et al, 2023) and fuel consumption (Chen, Lam, & Xiao, 2023; Uyanık et al., 2020; Zhang, Tsoulakos, Kujala et al, 2023). They may be combined by utilizing advanced AI methods training physics-based idealisations using comprehensive big data sets. Such predictions may enable ship operators to make informed decisions and minimize the ecological footprint of fuel-efficient shipping operations.

This chapter introduces an AI-based digital twin designed for enhancing the safety and sustainability of ship operations. In Section 2, an overview of digital twin models applicable to maritime operations is presented. The AI-based digital twin comprises of two layers, with the primary objectives to estimate ship fuel consumption and predict ship motions (Section 2 for further details). To evaluate and demonstrate the practical application of this approach, full scale measurement data is utilized, focusing specifically on a bulk carrier and a RoRo/Passenger ship (RoPax) (see Sections 4 and 5). Section 6, highlights the promising prospects of AI-based digital twins in the realm of developing intelligent decision support systems and for effectively monitoring ship safety and efficiency.

Figure 1. The ship digital twin for proactive optimization of ship operations

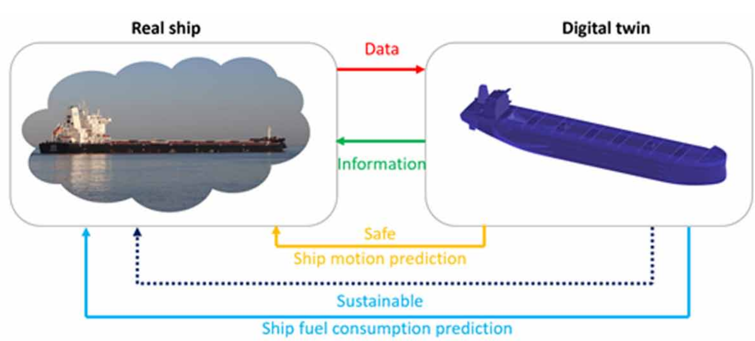

AN OVERVIEW OF DIGITAL TWIN MODELS FOR USE IN MARITIME OPERATIONS

Ship operations relate to seakeeping and ship performance in adverse conditions (Hirdaris & Mikkola, 2021). Models that may be used for the estimation of ship fuel consumption or seakeeping can be broadly classified into two categories namely (a) physics-based models and (b) Artificial Intelligence (AI) models.

In the area of ship efficiency, physics-based models can approximately estimate ship fuel consumption based on key assumptions that utilize the relationship between ship resistance and engine power (Kim et al., 2023; Tillig & Ringsberg, 2019). The estimation of fuel consumption is achieved via ship - propeller - engine performance models (Vitali et al., 2020). To accurately assess the total resistance experienced by a ship, both calm water and added resistance are considered (Kim et al., 2023; Lang, 2023). The physics-based models entail accounting for various components, including frictional resistance, the resistance of appendages, wave resistance of the bare hull and bulbous bow, as well as additional resistance arising from the immersed transom and model-ship correlation (Molland et al., 2017). In most cases, physics-based models have been employed to estimate ship resistance in still water. Empirical methods proposed by the International Towing Tank Conference (ITTC) have been widely utilized (ITTC, 2002). The Holtrop-Mennen model-based methods have also been used at the preliminary design stage (Holtrop & Mennen, 1982). In recent years, Computational Fluid Dynamics (CFD) has been utilized in detailed design (Campbell et al., 2022). Empirical methods can be utilized to estimate the added wave resistance (Hasselmann et al., 1973; Luo et al., 2016). To account for the effects of wave-induced added resistance and ship motions, semi-empirical models have been proposed. These models are based on experimental data and incorporate empirical equations to estimate added resistance in waves (Liu & Papanikolaou, 2020; Liu et al., 2016) and added resistance attributed to ship motions (ITTC, 2014; ITTC, 2017). Ship propulsion systems are often analysed using ship-propeller-engine performance models or simplified models based on the law of resistance transfer (Wang, 2020). However, their accuracy may be limited when dealing with complex operational conditions (Fan et al., 2022; Yan et al., 2021).

Artificial Intelligence (AI) methods offer a potential solution to overcome the challenges associated with physics-based models by leveraging big data to elucidate the intricate relationship between measured ship fuel consumption and a multitude of influential parameters (e.g., ship mechanical data and dynamics, main engine characteristics, weather conditions, and other relevant factors) (Chen, Lam, & Xiao, 2023). Review papers that discussed the potential application of AI methods in predicting ship fuel consumption (Fan et al., 2022; Yan et al., 2021), identify three main clusters of commonly utilized methods namely: (i) supervised machine learning (Coraddu et al., 2017), (ii) unsupervised machine learning (Hu et al., 2019), and (iii) deep learning (Kim et al., 2021). These methods may utilize diverse data sources and their combinations, such as voyage reports, Automatic Identification System (AIS), meteorological, and sensor data (Du et al., 2022). Diverse data sources enable accurate predictions. These algorithms can be used to predict ship fuel consumption based on well-defined scenarios for a specific ship. However, they often struggle to accurately predict real-time ship fuel consumption for an entire ship voyage under complex operational conditions. This is because traditional machine learning/deep learning methods may not effectively deal with complex influencing factors and make informed predictions of ship fuel consumption.

A digital twin may be utilized to closely monitor seakeeping and maneuvering, especially during challenging operational conditions (Lee et al., 2022; Major et al., 2021; Schirmann et al., 2018). For example, research in big data science has the potential to predict hydrodynamic derivatives by utilizing results from model tests or full scale measurements data. To date parametric estimation methods have been employed to quantify ship motions, relying on available ship mathematical models to train large data streams. For example, Wang et al. (2019) utilized the nu-support vector machine to identify hydrodynamic derivatives of the 3-DoF Abkowtiz model. Zeng et al. (2021) employed the Extended Kalman Filter (EKF) method to determine the hydrodynamic derivatives of an MMG model (Zeng et al., 2021). Non-parametric estimation models, such as Artificial Neural Networks (ANN) (Silva & Maki, 2022), Long Short-Term Memory (LSTM) 43, Gaussian process regression (Ouyang & Zou, 2021), and locally weighted learning methods (Woo et al., 2019), utilize simulated free-running tests to predict ship motion dynamics. Notably, Lou et al. (2022) developed neural network models to predict the motions of unmanned surface vehicles based on results from open seas manoeuvrability tests in 3-DoF.

The critical review of methods for the ship digital twins in ship operations indicates that existing digital twin models have their limitations. A common challenge is the accuracy of the digital twin representation. While digital twins aim to replicate physical objects or systems, there may still be discrepancies due to limitations in data collection, model accuracy, or real-time updates. For example, accuracy in terms of visualisation can be compromised because of the limited ability of parametric or non-parametric statistical regression models to consider medium to long-term environmental conditions. A high-fidelity digital twin requires careful calibration, validation, and continuous improvement to ensure reliability and accuracy.

MULTI-OBJECTIVE AI-BASED DIGITAL TWIN MODELS FOR SAFE AND SUSTAINABLE SHIP OPERATIONS

The digital twin presented in this chapter encompasses two essential deep learning layers, each serving a distinct purpose in enhancing ship operations. Figure 2 represents the architecture of the digital twin models, illustrating the integration of bi-directional Long Short-Term Memory (Bi-LSTM) with an attention mechanism layer for the prediction of ship efficiency and a transformer layer for the identification of ship motions.

Layer 1 focuses on idealizing the ship energy systems and predicting fuel consumption [12]. This layer can accurately estimate the ship fuel consumption in various operating scenarios. It considers ship operational characteristics (ship speed, draft, trim, etc.), and the influence of environmental conditions (wind, wave, and current, etc.). Predictive analytics may be crucial for ship operators who seek to optimize fuel usage, reduce costs, and decarbonise fleet operations.

Layer 2 can be used to understand and optimise seakeeping behaviour in real conditions [9]. Ship motions may influence ship stability, safety, and cargo integrity. Hence, the transformer integrated into this layer is trained using collected datasets that capture the complex relationships between various ship systems and operational factors (e.g., rudder angle, propeller rpm, speed, heading, weather condition) that may impact ship motions in 6 Degrees of Freedom (DoF) and in real-time. In this case, predictive analytics can enable ship operators to proactively respond to potentially hazardous conditions (e.g., ship–ship collision and ship grounding), adjust navigation strategies, and ensure ship safety.

Layer One: A Digital Twin Model for Fuel Efficiency Estimation

This section introduces the deep learning model based on Bi-LSTM with attention mechanisms [12], depicted in Figure 3. The model combines the strengths of Bi-LSTM, which can capture both past and

Figure 2. The overall procedure of AI-based ship digital twin

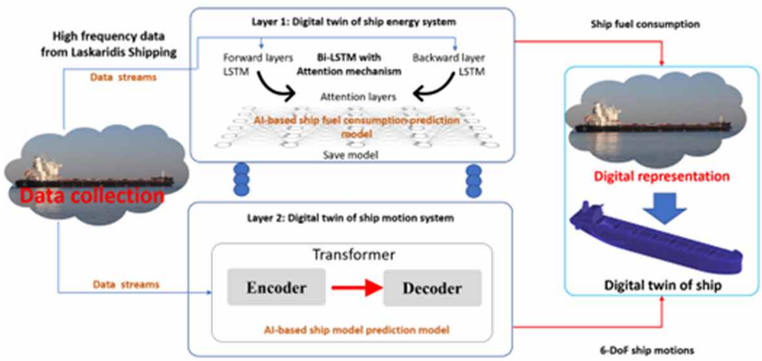

Figure 3. The schematic of AI based digital twin of ship energy system

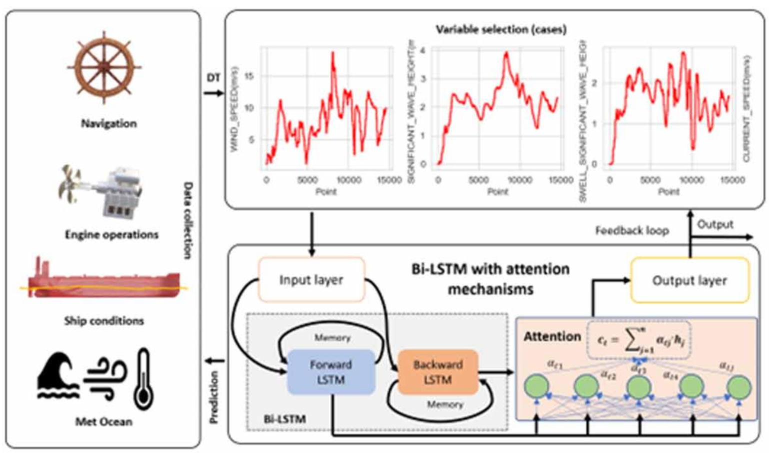

Table 1. Algorithm one: Bi-LSTM with attention mechanism for ship fuel consumption prediction

Input: Data collection SFC(n), see more in Section 2.1
Output: AI-based ship fuel consumption surrogate model
Select key variables X(n) and ship fuel consumption SFC (n) in the time domain
Split the training data set $data_{train}$ and $data_{test}$ from X(n) using k folds cross-validation method.
For batch $data_{batch\ size}$ in $data_{train}$
For L-length data $data_l$ in $data_{batch\ size}$
For $\boldsymbol{i} = 1$ to L
Using forward LSTM to an encoder $\overrightarrow{h_t}$
Using backward LSTM to an encoder $\overleftarrow{h_t}$
End For
Compute Attention score αi and ct
Compute ship fuel consumption SFCt from ct
End For
Training the model to identify ship energy system in real operational conditions
End For
Save the prediction model: AI-based ship fuel consumption prediction model

future dependencies, with attention mechanisms that enable the model to focus on relevant parts of the input data streams. Table 1 provides a summary of the algorithm, outlining the step-by-step procedure followed, including data pre-processing, model architecture setup, training process, and prediction generation. The architecture of the system, as illustrated in Figure 4, comprises four main components namely: (i) input layers, (ii) Bi-LSTM layers, (iii) attention layers, and (iv) the output layer.

The layers of the deep learning model are summarized as follows:

The **input layers** accept key variables obtained from navigation data, engine operation data, ship condition data, and hydrometeorological conditions from full scale measurements. Then these selected variables are pre-processed and fed into the subsequent layers.

Each **bi-LSTM layer** consists of two LSTM sublayers. Each LSTM unit comprises 4 interconnected elements, including the input and control signals for the input, forgotten, and output gates [45]. These components work together to regulate memory storage, retention, and output. Figure 4 depicts the internal structure of the LSTM unit (see red box). The input x_t at a time increment *t* and the output h_{t-1} of the hidden layer neuron at a time increment t-1 represent the joint inputs to the hidden layer. These inputs are then multiplied by distinct weight vectors, and upon application of the activation function, the control signals f_t, i_t, o_t, of the forgotten gate, input gate, and output gate are generated. This process is represented by Eqs. (1-3), where the weight vector is denoted by *w* and the activation amount by *b*. The biases for different connection weights are represented by b_f, b_i, and b_o, and σ(•)is the sigmoid activation function.

$$f_t = \sigma(\mathrm{w}f_{[}\mathrm{h}t_{-1,}\ \mathrm{x}t_{]} + \mathrm{b}f_{)} \tag{1}$$

$$i_t = \sigma(\mathrm{w}i_{[}\mathrm{h}t_{-1,}\ \mathrm{x}t_{]} + \mathrm{b}i_{)} \tag{2}$$

$$o_t = \sigma(\mathrm{w}o_{[}\mathrm{h}t_{-1,}\ \mathrm{x}t_{]} + \mathrm{b}o_{)}\ o_t = \sigma(w_o\left[h_{t-1}, x_t\right] + b_o) \tag{3}$$

The state of a cell $\tilde{C}_t$ is presented as per Equation (4). The value of the memory unit C_t is updated as per Equation (5). Accordingly, the output of hidden layer neurons h_t can be presented as per Equation (6)

$$\tilde{C}_t = \tanh(w_C\left[h_{t-1}, x_t\right] + b_C) \tag{4}$$

$$C_t = f_t C_{t-1} + i_t \tilde{C}_t) \tag{5}$$

$$h_t = o_t \tanh(C_t) \tag{6}$$

where tanh(•)represents a hyperbolic tangent activation function.

Ships are systems of systems that navigate through complex operational conditions (Zhang et al., 2021). To effectively capture the complexity of ship systems using real operational data for ship fuel

Figure 4. The architecture of Bi-LSTM with attention mechanisms

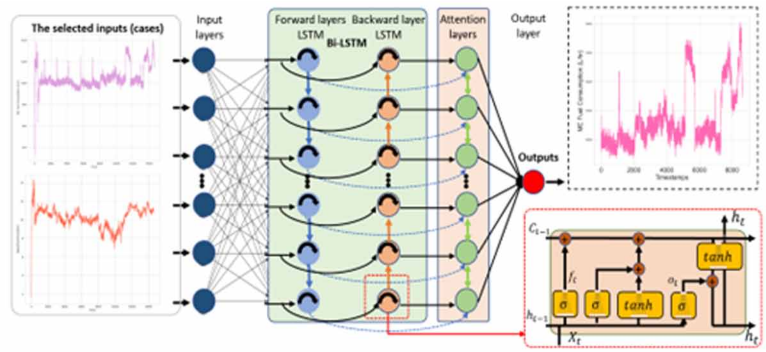

Figure 5. Capturing and utilizing information from both forward and backward directions

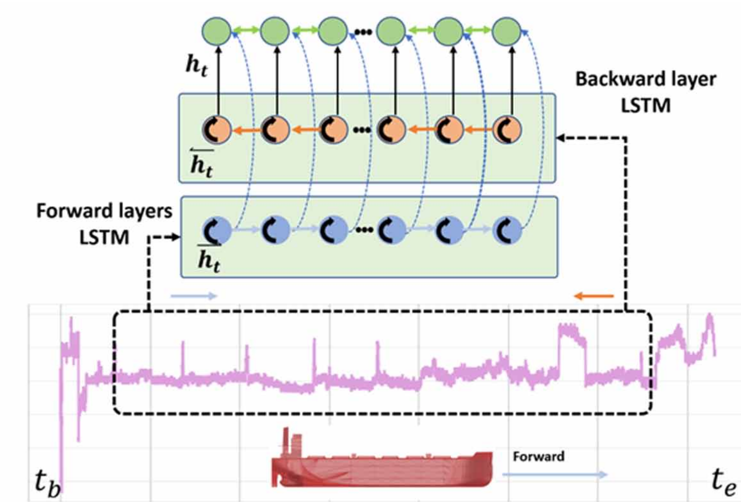

consumption prediction, it is essential for the model to learn from both past and future information in the data streams. While a standard LSTM model only considers information from past time frames in the data stream, the bi-LSTM layer overcomes this limitation by addressing the problem of disregarding relevant past information (Ma et al., 2022). This is because it comprises both forward and backward LSTM sublayers, see Figure 4. Forward sublayers process the input stream in a forward direction i.e., from the beginning t_b to the end t_e. In a backward direction the sublayers operate from the end t_e to the beginning t_b, see more in Figure 5.

A bidirectional LSTM processes input data stream in both forward and backward directions. By concatenating the outputs of the forward and backward LSTMs, the model could obtain a representation that incorporates both past and future information, as shown in Figure 5. Given an input data stream $X=[x_1,x_2,\ldots,x_n]$, a bidirectional LSTM generates hidden states in both forward and backward directions as shown in Eqs. (7-8). The hidden states from both directions are concatenated to obtain a comprehensive representation at each time step as Equation (9).

$$\overrightarrow{h_t} = \mathrm{LSTM}\left(x_t, \overrightarrow{h_{t-1}}\right) \quad (7)$$

$$\overleftarrow{h_t} = \mathrm{LSTM}\left(x_t, \overleftarrow{h_{t-1}}\right) \quad (8)$$

$$h_t = \left[\overleftarrow{h_t}, \overrightarrow{h_t}\right] \quad (9)$$

where *t* represents the time step, and $\overrightarrow{h_t}$ is the hidden state in the forward direction. $\overleftarrow{h_t}$ is the hidden state in the backward direction, [;]denotes the concatenation.

The **attention mechanism** allows the model to dynamically focus on different parts of the input data streams, thus assigning varying levels of importance to different time steps [9]. This enhances the ability to emphasize critical information from data streams, which is useful to capture extreme scenarios of ship operations in real complex operational conditions. The attention layers calculate attention scores and weights for each time step based on the hidden representations from the Bi-LSTM layers, as shown in Figure 6.

Given a specific time step *t*, the attention weight αt_j of other hidden layers for the current input for x*t* is calculated as Equation (10). The alignment score et_j computed using a trainable alignment model is defined as Equation (11). The context vector c*t* is the weighted sum of the hidden states, which reflects the attended information at time step t as Equation (12). The final output S*FCt* at time step t is generated by passing the context vector c*t* through a linear transformation and an activation function as Equation (13).

Figure 6. Attention mechanism for the prediction of ship fuel consumption

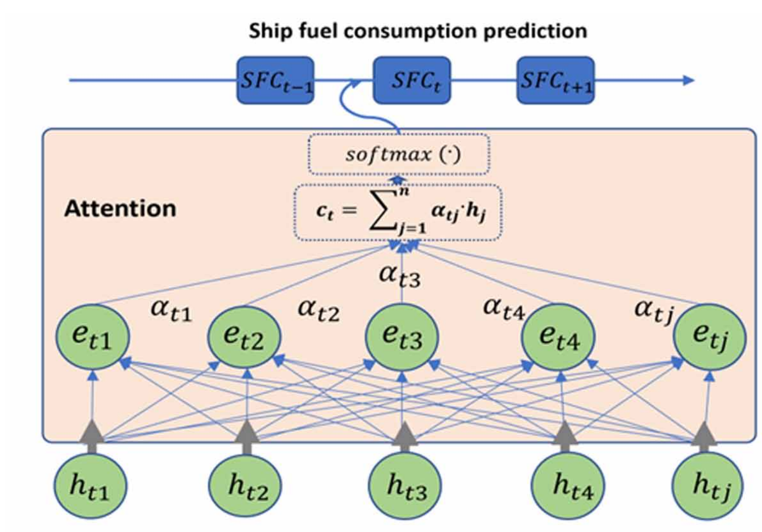

$$\alpha_{tj} = \frac{\exp\left(e_{tj}\right)}{\sum_{j=1}^{n}\exp\left(e_{tj}\right)} \tag{10}$$

$$e_{tj} = w_{\mu}^{T} * tanh(w_w h_t + b_w) \tag{11}$$

$$c_t = \sum_{j=1}^{n} \alpha_{tj} h_j \tag{12}$$

$$SFC_t = softmax(W_c \cdot c_t + b_c) \tag{13}$$

where, W_c, and b_c are parameters (weight matrices or vectors) that are typically trained and determined during the process of model training.

(iv) The **output layer** receives the context vector, which is the weighted combination of the hidden representations obtained from the attention layers. The context vector captures the most relevant information from the input data stream. The output layer processes the context vectors and predicts the ship fuel consumption for the given time step, see Figure 6.

Layer Two: A Digital Twin for the Prediction of Ship Motions

The transformer is an advanced deep learning architecture that utilizes self- and multi-head attention mechanisms [9]. It enables the differential weighting of input features to determine their importance. This section introduces a transformer-based digital twin of the ship motion system. A transformer-based deep learning method is employed to train ship trajectory data streams and make long-term ship motion predictions in the time domain. Figure 7 illustrates a ship trajectory with time series of ship motions influenced by environmental conditions that are used to train the model. Each point on the trajectory includes ship control actions, desired inputs, environmental conditions, and 6-DoF ship motions. The model can identify and forecast 6-DoF ship motions as shown in Figure 8. The transformer architecture, illustrated in Figure 9, consists of encoder and decoder modules, each containing multiple blocks represented by grey areas (Han et al., 2021).

The encoder module incorporates multi-head attention and a feed-forward neural network, enabling the mapping of time series data related to operational conditions, control devices, and desired inputs (see $\boldsymbol{X}$ in Equation (14)) to a new continuous series ($\boldsymbol{Z}$ in Equation (15)), see Figure 8. This mapping is achieved via an "attention mechanism" defined by the *SoftMax* function in Equation (19). The objective is to predict the time series of ship motions ($\boldsymbol{Y}$ in Equation (16)) using an autoregressive method. The attention mechanism employed in the digital twin model facilitates the retention of crucial information during the training and prediction of significant data streams [49].

$$\boldsymbol{X} = \{x_1, x_2, x_3, \ldots, x_n\} \tag{14}$$

Figure 7. 6-DoF ship motion dynamics along ship trajectory

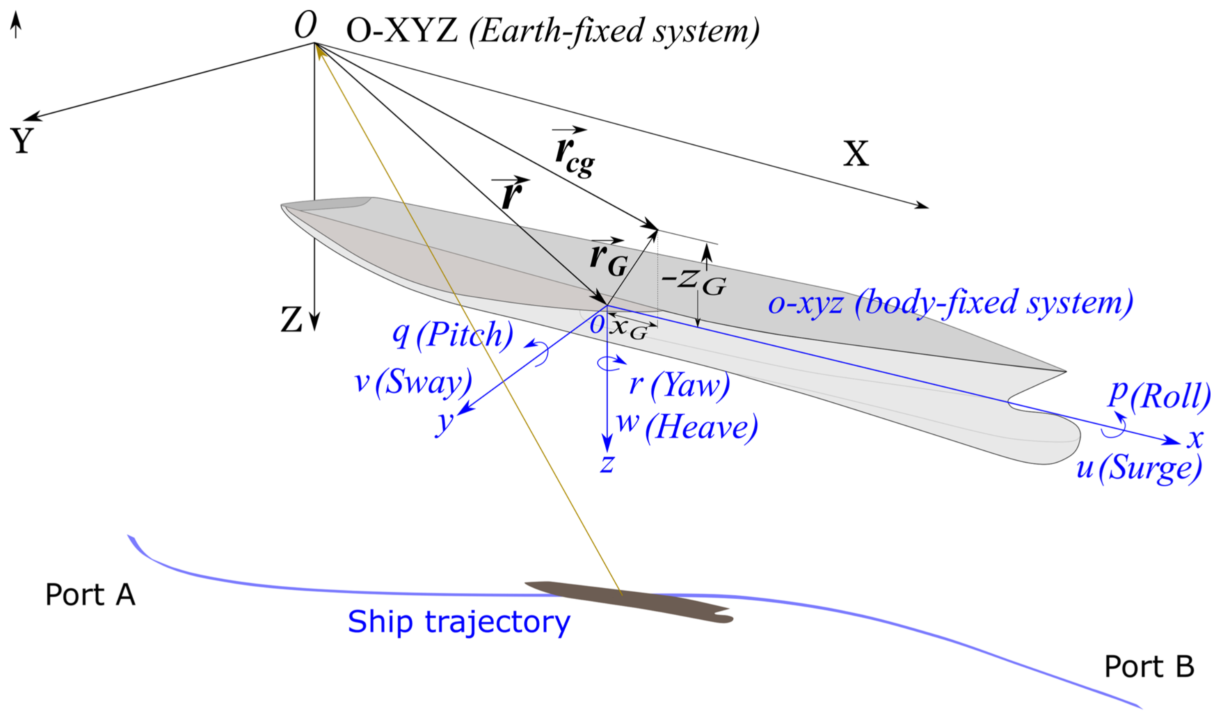

$$\boldsymbol{Z} = \{z_1, z_2, z_3, \ldots, z_n\} \tag{15}$$

$$\boldsymbol{Y} = \{y_1, y_2, y_3, \ldots, y_n\} \tag{16}$$

where, $\boldsymbol{X}$ denotes the matrix of control devices, conditions, and desired inputs in the time domain; $\boldsymbol{Y}$ denotes the matrix of the 6-DoF ship motion in the time domain; $\boldsymbol{Z}$ denotes a matrix after encoding; x_n denotes the inputs of control devices, conditions, and desired inputs at point n; y_n denotes the outputs of 6-DoF at point n.

Figure 9 presents a deep learning network consisting of an encoder and decoder, both composed of multiple layers of attention. The network aims to process and analyse training data streams of ship motions. Initially, the ship motion data is fed into an "Input Embedding layer", which treats the data as a lookup table to generate a learned vector representation of ship motions. A feed-forward neural network layer then learns the number of lookup tables from the training database, allowing the ship motion data streams from different ship trajectories to be organized into vectors. To account for variations over sea depth and across a trajectory, a smart positional encoding scheme is employed to incorporate positional information of data streams into the vectors from the Input Embedding layer [48,49]. This encoding process is defined mathematically by Eqs. (17)-(18) (Vaswani et al., 2017). The input vectors, resulting from the embedding and positional encoding of ship motion data, are combined and used to train the encoder and decoder modules of the model [9].

Figure 8. Transformer architecture for ship motion prediction

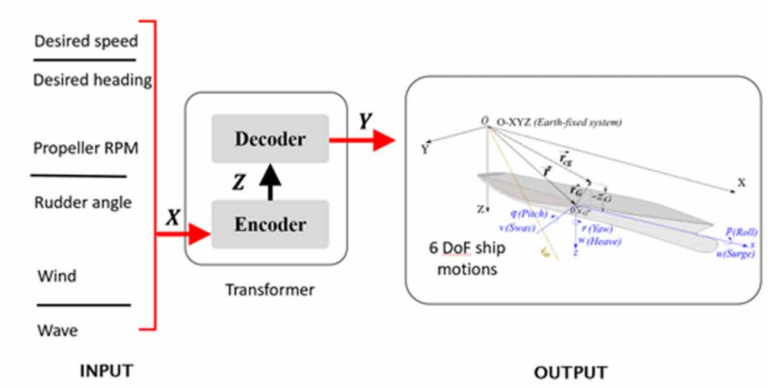

$$PE_{(pos,2i)} = \sin\left(pos / 10000^{2i/d_{\text{model}}}\right) \tag{17}$$

$$PE_{(pos,2i+1)} = \cos\left(pos / 10000^{2i/d_{\text{model}}}\right) \tag{18}$$

where, *pos* denotes the location of the time series of ship motions, and *i* presents the dimensionality of d_{model}.

Figure 9. Transformer architecture for 6-DoF ship motion prediction

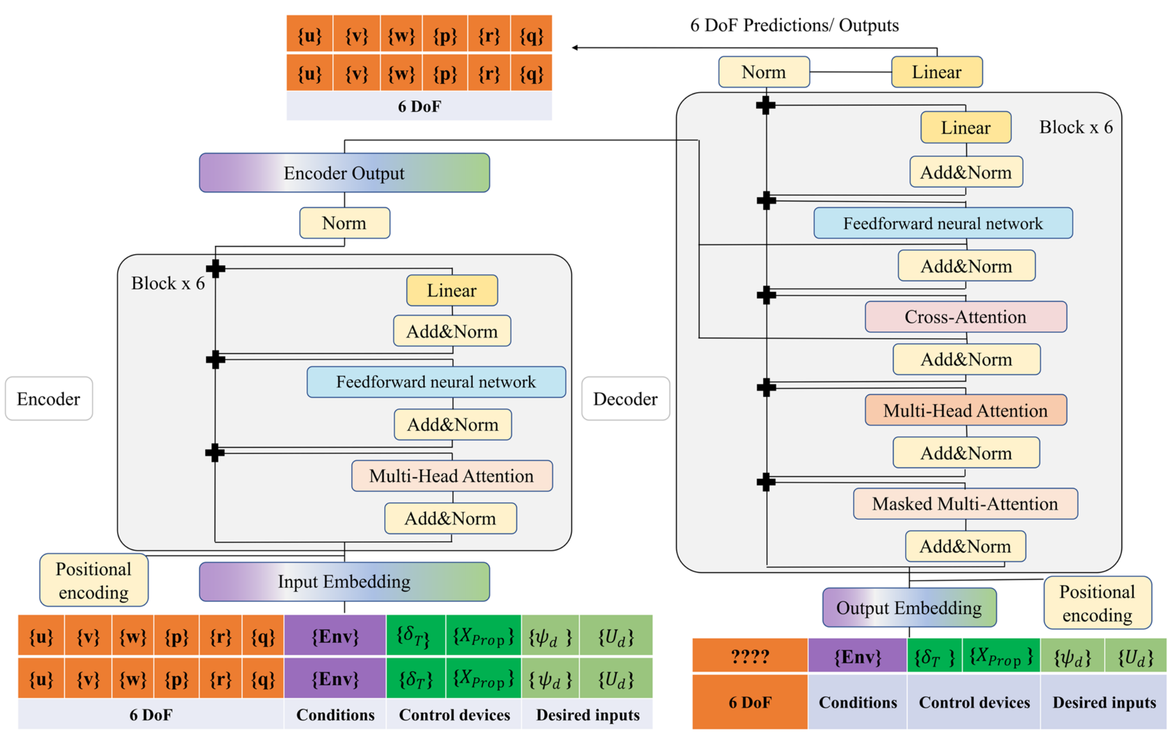

Once the vector with positional encoding is passed to the encoder and decoder modules (Figure 9), the encoder module is employed to map the input time series to a set of new continuous series. The decoder module utilizes an auto-regressive technique to generate the output time series for ship motion prediction, see Eqs. (14)-(16). Both the encoder and decoder consist of similar sub-layers. As illustrated in Figure 9, the encoder and decoder modules encompass the following components: (1) Attention mechanism/multi-head attention/marked multi-head attention layer; (2) Add & Norm function layer; (3) Feed-forward networks (FFN) layer; and (4) Linear layer [9].

(1) Attention mechanism / multi-head attention layer

The attention mechanism in the deep learning model provides exceptional long-term memory for ship motion time series, allowing the model to attend to and focus on the ship motion information during the entire voyage. The attention layer and SoftMax functions are defined based on Equation (19) in the transformer architecture, as described in Vaswani et al. (2017).

$$z = Attention(Q,K,V) = SoftMax\left(\frac{QK^T}{\sqrt{d_k}}\right)V \tag{19}$$

where Q, K, and V are query, key and information value vectors,

$$Q \in R^{n\times d_k}, K \in R^{m\times d_k}, V \in R^{m\times d_v}$$

are the matrixes, including query, key, and value of attention; d_k denotes the dimensions in blocks. $Q=X\times QW$, $K=X\times KW$, $V=X\times VW$. QW, KW, and VW are weight matrices; z denotes an element of the matrix Z which is calculated using *SoftMax* functions.

Each attention process in this model functions as a learning mechanism for ship motions. Multiple attention heads can predict output vectors, which are then concatenated into a single output vector. This multi-head attention approach enables the learning of more comprehensive information about ship motions compared to a single attention layer. The multi-head attention layer consists of individual attention layers as denoted in Eqs. (20)-(21). The marked multi-head attention layer represents a hidden layer within the multi-head attention. The use of a mask indicates a matrix that scales the attention scores of the multi-head attention layer, as further detailed in Bhattacharya et al. (2022) [51].

$$\text{MultiHead}(Q,K,V)= \text{Concat}(head_1,\ldots,head_h)W^O \tag{20}$$

$$head_i = Attention\left(QW_i^Q, KW_i^K, VW_i^V\right) \tag{21}$$

where, $W^o \in R^{h\times d_{model}\times d_k}$, h denotes the number of parallel attention layers. QW, KW, and VW are weight matrices, $W_i^Q \in R^{d_{model}\times d_k}, W_i^k \in R^{d_{model}\times d_k}, W_i^v \in R^{d_{model}\times d_k}$.

(2) Add & Norm layers

To incorporate the output vector from the hidden multi-head attention layer with the original positional input embedding of the ship's time domain motion, Add & Norm layers are utilized. The Add layer consists of a residual network or residual connection, which enables the learning of residual functions for the inputs, as shown in Equation (22). The output of the Add layer then passes through a Norm layer, which applies layer normalization to enhance performance and training efficiency, as described in Eqs. (22)-(25). These layers facilitate the integration and normalization of the input and output vectors in the model.

$$F(x) = \mathrm{H}(x) - x \tag{22}$$

$$\mu^l = \frac{1}{h}\sum_{i=1}^{h} a_i^l \tag{23}$$

$$\sigma^l = \sqrt{\frac{1}{h}\sum_{i=1}^{h}(a_i^l - \sigma_\mu^l)^2} \tag{24}$$

$$\widehat{a^l} = \frac{a^l - \sigma_\mu^l}{\sqrt{\left(\sigma^l\right)^2 + \mu}} \tag{25}$$

In the above equations $H(x)$ is the desired mapping, $F(x)$ denotes the stacked nonlinear layers, and the original mapping reconstructed as $F(x)+x$; h denotes the number of nodes of the hidden layer; l denotes the number of layers. The σ^l and μ^l are the parameters of layer normalization; σ_μ^l is the mean value; $\widehat{a^l}$ denotes the results of layer normalization and ε denotes a very small number that can be used to avoid $\sqrt{\left(\sigma^l\right)^2 + \mu} = 0$, see Equation (25).

(3) Feed-forward network

The output from the Add & Norm layers is then passed through feed-forward networks for additional processing. The Feed-Forward Network (FFN) is employed to enhance network stability and reduce training time. It consists of multiple linear layers, with a Rectified Linear Units (ReLU) activation function, connecting each sub-layer. Further details can be found in the work by Li et al. (2019).

$$FFN(x) = \max(0, xW_1 + b_1)W_2 + b_2 \tag{26}$$

$$ReLU(x) = (x)^{+} = \max(0, x) = \begin{cases} x & if \quad x > 0 \\ 0 & if \quad x \leq 0 \end{cases} \tag{27}$$

where, the function max () denotes the ReLU function as per Equation (27); W_1, and W_2 represent the value of slope; b_1, and b_2 represent the value of intercept.

(4) Linear layer

The decoder is capped off with a linear layer that acts as a classifier to present the predicted outputs. The linear function is the linear transformation of data streams [50]

$$y = xA^T + b \tag{28}$$

where, A^T represents the value of slope; b represents the value of intercept.

The complex architecture of the transformer allows learning different ship motion dynamics in real conditions, potentially boosting the predictive ability of the ship manoeuvring features of the selected ship, see testing and validation in Sections 4.2 and 5.2. To evaluate the performance and quantify the errors between the real and digital twin, Root Mean Square Error (RMSE), Mean Square Error (RMSE), and error rate e_n are used as shown in Eqs. (29-31).

$$RMSE = \sqrt{\frac{1}{N}\sum_{n=1}^{N}(y_n - \hat{y}_n)^2} \tag{29}$$

$$\mathrm{MSE} = \frac{1}{N}\sum_{n=1}^{N}(y_n - \hat{y}_n)^2 \tag{30}$$

$$e_n = (y_n - \hat{y}_n) / (y_n) \tag{31}$$

where, y_n is the actual value, $\hat{y}_n$ denotes the predicted value, $\overline{y_n}$ is the mean value.

AI-Based Digital Twin Models

This section demonstrates the use of multi-objective AI-based digital twin models [9, 12]. Layer 1 of the digital twin model is trained by utilising extensive data streams derived from high-frequency full scale measurements data of a Kamsarmax bulk carrier owned by Laskaridis Shipping Co. Ltd. (see Table 2). Figure 10 illustrates voyages from full scale measurements data collected for this vessel from February 2021 to February 2023. Layer 2 of the digital twin model was trained using operational data obtained from the Ro-Pax ship owned by Viking Line Co. Ltd (see Table 3). Trajectories and hydro-meteorological

Table 2. Ship specification of the KAMSARMAX class bulk carrier

Information		Real
IMO	9843405	
Vessel Type	Bulk Carrier	
DWT	81 600.0 t	Digital Twin
Length x Breadth	229.0 x 32.0 m	
Year Built	2020	

Figure 10. Full scale measurment data of the selected bulk carrier from 02.2021 to 02.2023

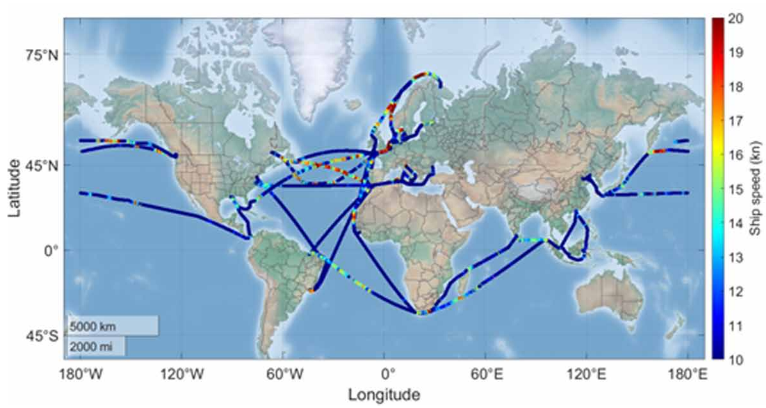

Table 3. The ship specification of the selected Ro-Pax ship

Information		Real
IMO	9773064	
Vessel Type	Ro-Pax ship	
DWT	49 134.0 t	Digital Twin
Length x Breadth	212.0 x 30.6 m	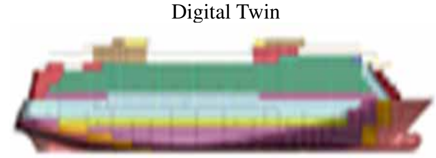
Year Built	2017	

Figure 11. Ship voyages from Helsinki to Tallinn

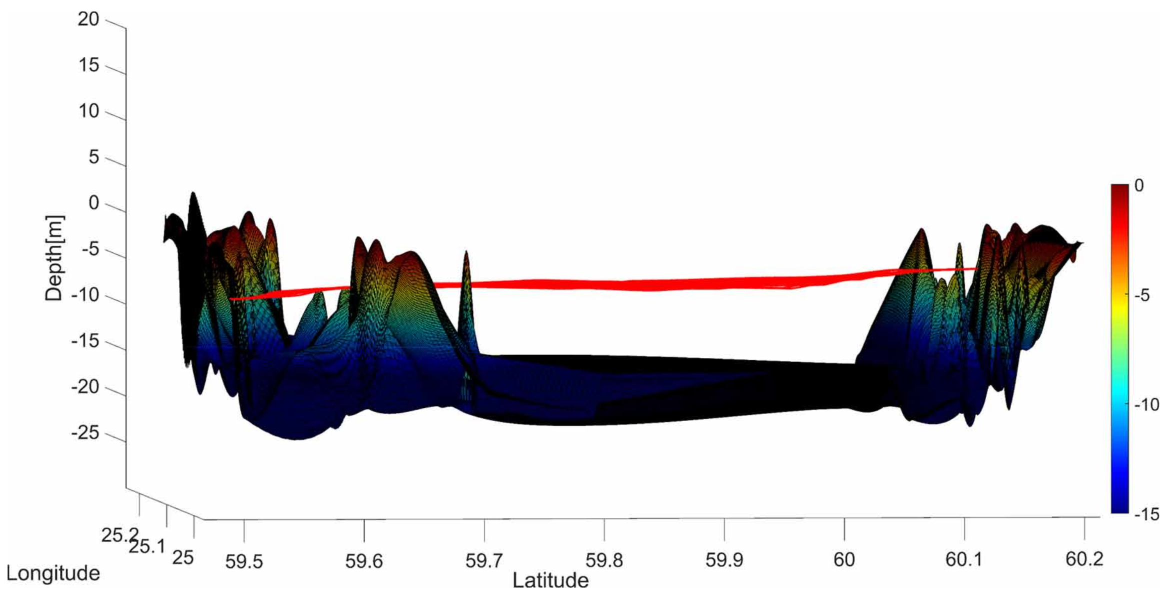

conditions were observed between two ports situated in the Gulf of Finland as shown in Figure 11 [9]. This approach was adopted due to the inherent challenge of collecting all the required data from a single ship.

Ship Fuel Consumption Predictive Analytics

A bi-LSTM architecture was employed to train a digital twin of the ship energy systems. Inputs to the model encompassed ship navigation data such as ship speed, course and heading, operational conditions (e.g., ship mean draft and trim, main engine shaft power and temperature), and Metocean data encompassing wave characteristics, wind conditions, current information, and air temperature. These inputs were carefully selected based on their relevance to fuel consumption prediction. The output of the model was the ship fuel consumption represented in the time domain. This information was utilized to drive the predictions generated by the digital twin A visual representation of the model architecture and its components can be found in Figure 12. To train the digital twin of the ship energy system, the digital twin of the ship energy system employed an architecture consisting of an input layer, three bi-LSTM layers, three attention layers, and an output layer. The bi-LSTM layer had 128 hidden units. The model characteristics and the selected hyperparameters are presented in Table 4.

The training loss and validation loss were calculated using the training (80%) and validation (20%) datasets, respectively. The curves shown in Figure 13 illustrate that both of those decrease and stabilize around the 178th epoch. Therefore, if no improvement in the validation performance is observed beyond this point, the training process is terminated early to prevent overfitting. After completing 178 epochs, the deep learning model achieves an optimal fitting state, indicating a balanced convergence between the model's performance and the training data. This optimal fitting state implies that the model does not suffer from overfitting, characterized by excessive complexity and high accuracy on the training data but poor generalization to testing data. It also avoids underfitting, which occurs when the model fails to capture underlying patterns in the data, resulting in subpar performance on both training and testing

Figure 12. The digital twin processing of ship fuel consumption prediction for model training, testing and application (Zhang, Tsoulakos, Kujala et al, 2023)

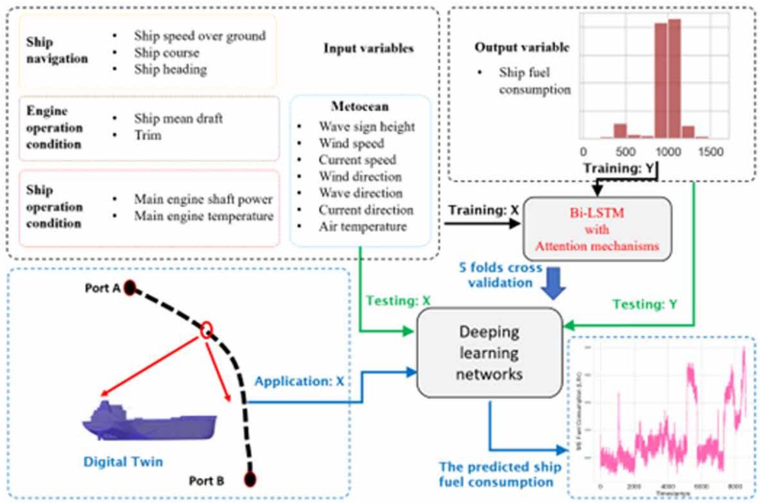

Table 4. The model characteristics and the optimal hyperparameters

Model	Input variables	output variable	layers
Bi-LSTM	14	1	7
Hidden units per layer	Optimizer	Batch Size	Early stopping
128	Adam	48	Patience=10
Dropout rate	Leaning rate	Epochs	Regularization param
0.2	5e-05	178	0.1

Figure 13. The model performance evaluation

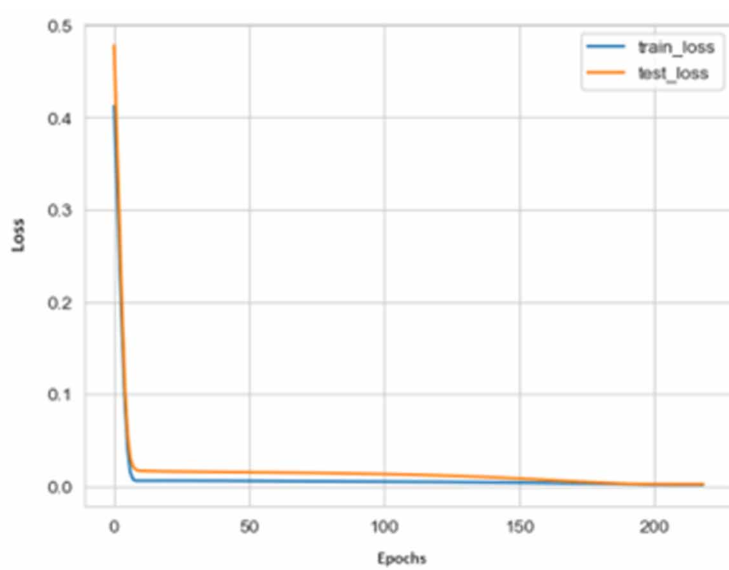

data. The digital twin of the ship energy system built using the deep learning model achieves a desirable equilibrium by effectively capturing the intricacies of the training data while also generalizing well to new data streams.

As depicted in Figure 13, the training process demonstrates that the deep learning model can achieve an optimal fit, effectively addressing both overfitting and underfitting. Furthermore, the average validation loss using Mean Squared Error (MSE) is determined to be 2.04e-2. To further evaluate the trained deep learning model, new inputs were selected from the testing database, as illustrated in Figure 12. The model was used to predict ship fuel consumption in the time domain, and the resulting error rates were calculated using Equation (31), as shown in Figure 14. The results of ship fuel consumption prediction are illustrated in the upper figure. The red line represents the real values of ship fuel consumption, while the green line represents the predicted results. The alignment and deviation between the two lines indicate the accuracy of the digital twin. In the bottom figure, the blue line represents the error rate in the time domain. It shows the magnitude and direction of the errors between the predicted and actual fuel consumption values at different points in time. These findings indicate that the trained deep learning model can effectively capture the characteristics of the ship energy system under real operational conditions. Further analysis of the prediction errors is presented in Figure 15. Over 90% of errors are below 4%, with an average error rate of 0.98%. It is important to note that the proposed model has limitations in effectively capturing abnormal fluctuations present in the sensor-collected data. This is also reflected in the significant errors indicated by the peak values in lower Figure 14.

Figure 15. The analysis of prediction errors using the proposed model

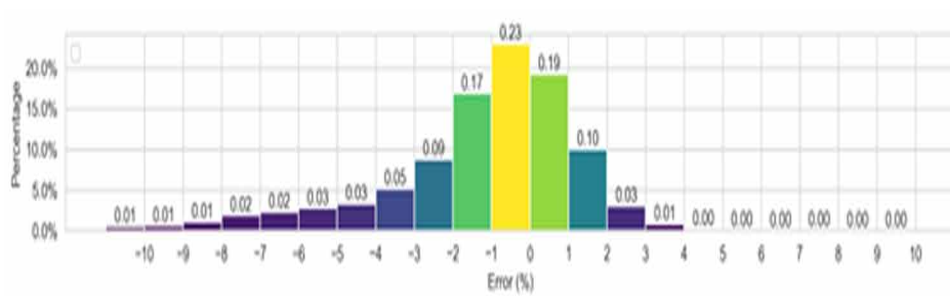

Figure 14. The comparison of real and predicted ship fuel consumption

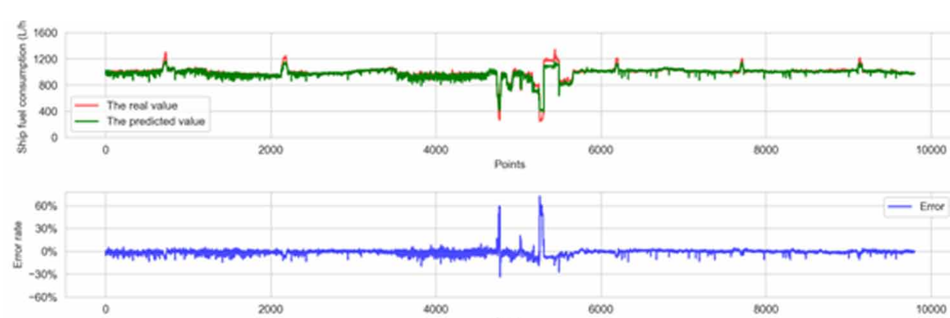

Ship Motions Predictive Analytics

For the typical Ro-Pax ship shown in Table 3, ship trajectories were collected during the ice-free period between 2018 and 2019. The waterway between Helsinki and Tallinn may freeze during the winter months of December, January, and February. However, this aspect is not considered in the present analysis.

A 6-DoF ship dynamics model (Taimuri et al., 2020) was utilized to generate time-domain input parameters (rudder angle, propeller rpm) and time-domain output results (6-DoF ship motion dynamics) for 500 voyages between Helsinki and Tallinn, see Figure 11. Subsequently, a transformer architecture was developed to train a deep-learning model that maps the inputs to the outputs. Inputs $\{X\}$ encompass rudder angle, propeller rpm, speed, heading, wind information, and wave information. Outputs $\{Y\}$ comprise surge, sway, heave, roll, pitch, and yaw. This information was employed to guide the predictions produced by the digital twin of the ship motion system. A visual representation of the model architecture and its components can be found in Figure 16. To capture the key features of historical ship motion dynamics, a complex architecture of the transformer was designed. Model characteristics and selected hyperparameters are presented in Table 5.

The total dataset comprised a total of 500 voyages divided into three parts: 80% for training (400 ship voyages), 10% for validation (50 voyages), and 10% (50 voyages) for testing. The curves shown in Figure 17 demonstrate that both the training and validation losses decrease and stabilize at the 38th epoch. The results of the training process indicate that the deep learning model achieves an optimal fit, indicating that it neither overfits nor underfits the data. To test the digital twin of the ship motion system, the future inputs of ship control actions, desired inputs, and environmental conditions were considered. The 6-DoF ship motions were then predicted, as depicted in Figure 18. The ground truth represents the

Figure 16. The digital twin processing of 6-DoF ship motion prediction for the long-term voyage in real conditions and turning circle in calm conditions (Zhang, Taimuri, Zhang et al, 2023)

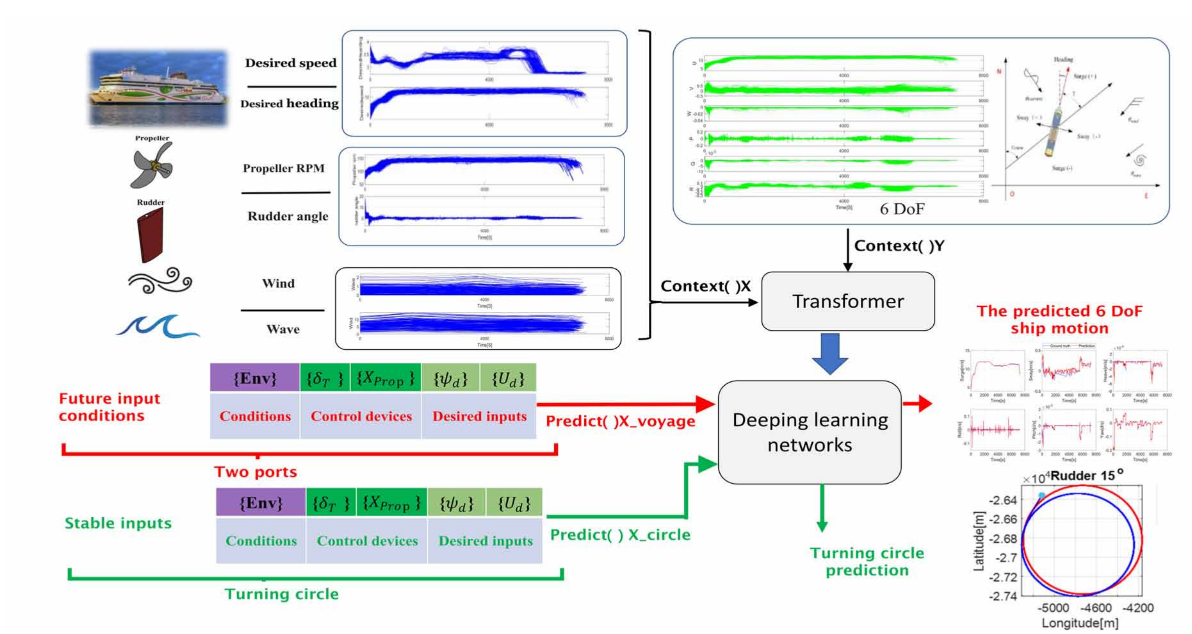

Table 5. The model characteristics and hyperparameters of the transformer

Model	Input variables	Output variable	Encoder
Transformer	8	6	6 blocks
Decoder	Optimizer	Batch Size	Dimension
6 blocks	Adam	8	256
Encoder	Encoder module	Inner layers	Epochs
1 parallel attention layer	3 parallel attention layers	1,024 dimensions	48

Figure 17. The model performance evaluation

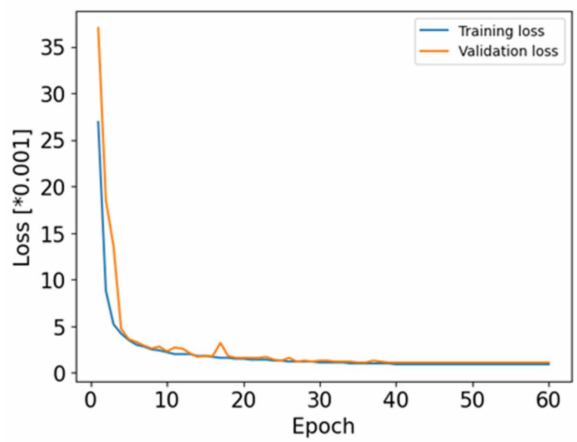

Figure 18. The comparison of real and predicted ship motions

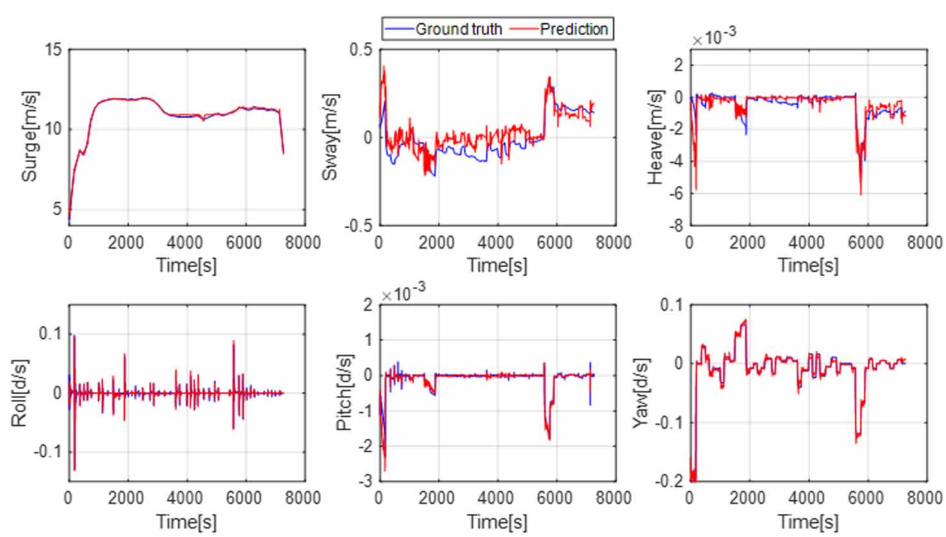

Figure 19. The results of the performance evaluation using R^2 value

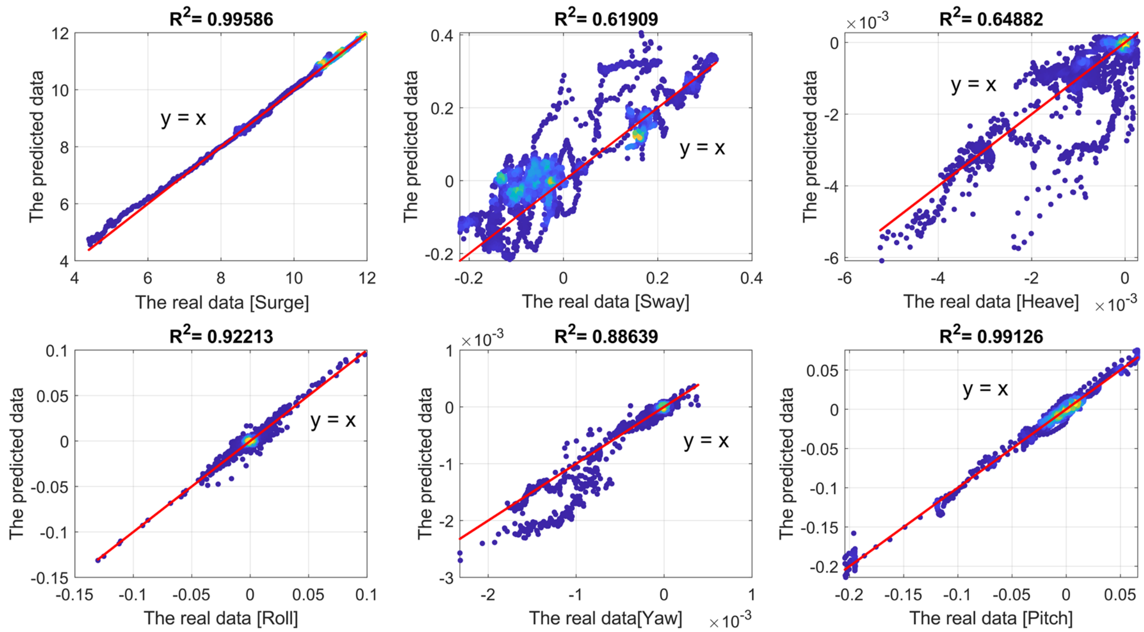

real data in blue. The prediction denotes the predicted results in red. These results demonstrate that the digital twin model can effectively capture the ship motion features in real-world conditions.

To accurately evaluate the performance of the trained model, R^2 values were calculated and assessed (Figure 19). The R^2 values for surge, roll, and pitch predictions exceeded 0.9, thus indicating a strong correlation between the predicted and real values. The R^2 values for sway and heave predictions are 0.62 and 0.65, respectively. These results suggest that the predicted and real values are in close agreement. The model demonstrated good performance in predicting all 6-DoF ship motions. However, the agreement for sway and heave predictions is slightly lower as compared to surge, roll, and pitch. This discrepancy may be attributed to the adopted method, which is based on an auto-regression model that may underestimate certain influential factors in ship sway and heave, such as swell, current, etc.

APPLICATIONS OF MULTI-OBJECTIVE AI-BASED DIGITAL TWIN MODELS

As a first step toward demonstrating the benefits of an AI-based digital twin in this section, the models outlined in Section 4 are utilized to predict ship fuel consumption and to estimate ship turning circles in calm sea conditions.

Ship Fuel Consumption Prediction

To expand the usage of the trained digital twin model to a subsequent voyage of the ship indicated in Table 2, which begins in Canada and ends at Attu Island as shown in Figure 20. The ship is operating in

Figure 20. Ship fuel consumption prediction by calling the trained digital twin model

```
Save model: model.save('Ship fuel consumption model.h5')
Load model: loaded_model = load_model('Ship fuel consumption model.h5')
Use the model: Predictions = loaded_model.predict(New_inputs)
```

a loaded condition, with a deadweight tonnage (DWT) of 76,528 metric tons, and the estimated distance of the voyage is approximately 3,994 nautical miles.

The error analysis of ship fuel consumption prediction for an entire voyage is presented in Figure 21. In the upper figure, the red line represents the real values of ship fuel consumption, while the green line represents the predicted results. In the middle figure, the blue line represents the error rate in the time domain. The bottom figure displays the prediction error distributions. It provides a visual representation of the distribution of errors across different ranges or intervals. Examining the error distributions can offer insights into the overall performance and identify any systematic biases or patterns in the prediction errors. The findings, unveil the outcome of the fuel consumption prediction using the trained digital twin. They highlight that more than 90% of the prediction errors are below 5%, and the average error of the ship fuel consumption of the whole voyage is measured at 2.54%. These results serve to affirm the viability of deploying the trained digital twin model as an efficacious tool for forecasting fuel consumption during comparable voyages. Consequently, the application of the model holds the potential to furnish valuable insights and facilitate efficient fuel management and optimization endeavours in real operational conditions.

Turning Circles Prediction Using the Digital Twin of the Ship Motion System

To demonstrate the generalization capability of the digital twin of the ship motion system, the prediction of ship motion dynamics was conducted by setting stable rudder angles as new inputs to generate turning circles. The selected stable rudder angles were set at 1°, 5°, 10°, and 15° (starboard), while the propeller revolutions were fixed at 109 rpm. Figure 22 illustrates the predicted turning circles for different rudder angles (1°, 5°, 10°, and 15°). The results indicate that the trained digital twin model can capture the turning characteristics of the ship accurately, despite not being explicitly trained on ship turning circle data. This suggests that the model has effectively "learned" the ship maneuvering features and can generalize well to new scenarios. Figure 23 presents an error analysis of turning circle predictions

Figure 21. The error analysis of ship fuel consumption prediction using the trained digital twin model

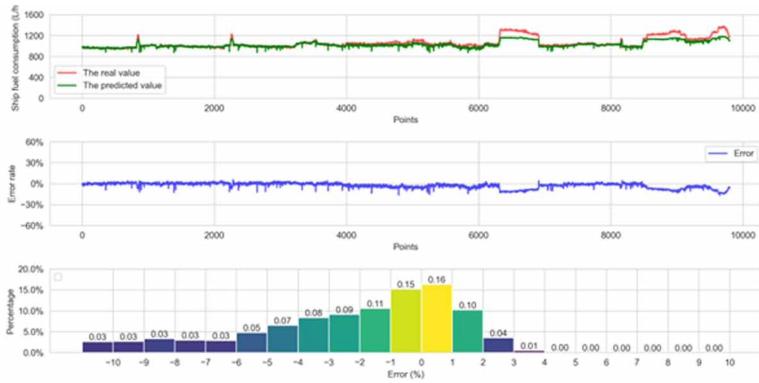

Figure 22. The prediction of the ship turning circle using the designed digital twin model

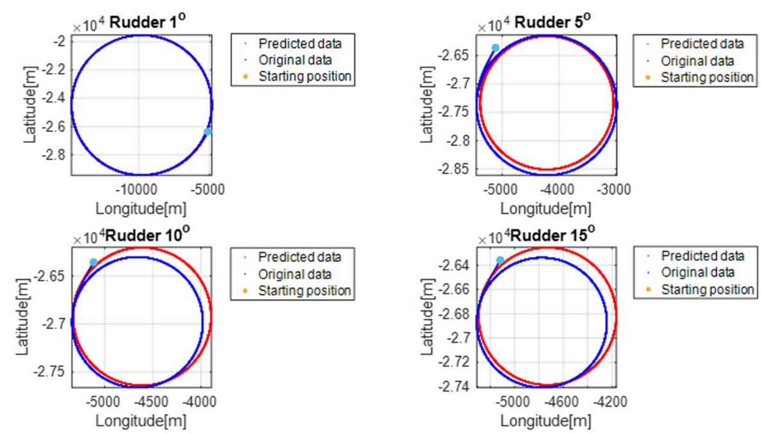

for various rudder angles (1°, 5°, 10°, and 15°). The analysis reveals that the predicted error increases as the rudder angle increases. This can be attributed to the fact that a significant majority (96.8%) of the rudder angles in the trained datasets fall within the range of -1° to 1°, as depicted in Figure 24. Consequently, as the rudder angle deviates from this range, the number of available training data points decreases, resulting in lower accuracy for turning circle predictions with higher rudder angles. To further improve the accuracy of the digital twin of the ship motion system in predicting turning circles for high rudder angles, it is suggested to train the model with more complex voyages that involve ship motion dynamics in real conditions. By incorporating such data into the training process, the model can learn to handle the complexities and variations associated with higher rudder angles, thereby enhancing its accuracy and performance.

Figure 23. The error analysis of turning circle prediction at different rudder angles

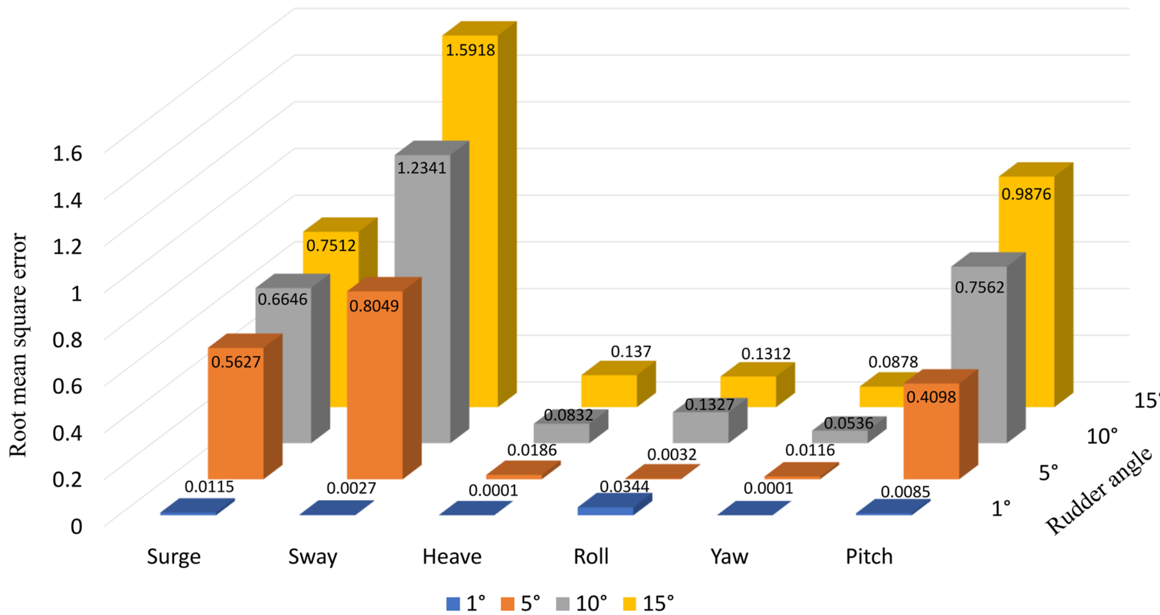

Figure 24. The distribution of the rudder angles of the trained data. The window demonstrates that distribution ranges from [-1 to 1]

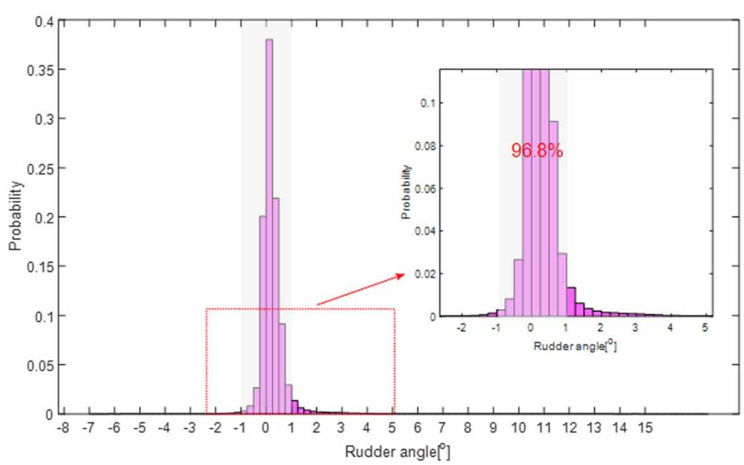

CONCLUSION

This chapter introduced a ship digital twin model designed to enhance safe and sustainable ship operations. The digital twin presented consisted of two distinct layers: (a) Layer 1 that incorporates a bi-directional LSTM network with attention mechanisms to replicate the ship's energy system and estimate ship fuel consumption in real operational conditions; (b) Layer 2 that employs a transformer neural network to construct a digital twin model of the ship's motion system, thus enabling analysis of ship motions in relation to hydro-meteorological conditions. The ship digital twin was trained, validated, and tested using bulk carriers and Ro-Pax ships as focal points. Key conclusions derived from the study can be summarized as follows:

The innovative use of multi-objective AI-based digital twin models for predicting ship motions and ship fuel consumption holds significant promise and utility in ensuring safe and sustainable ship operations.

High-frequency sea tail data streams are invaluable for constructing ship digital twins, and the proposed deep learning methods effectively capture the complex relationships between external conditions, internal conditions, and ship performance.

Layer 1 of the AI-based ship digital twin learns the ship's energy systems and can be utilized to estimate long-term ship fuel consumption under real operational conditions.

Layer 2 of the AI-based ship digital twin identifies the ship's motions accounting for realistic hydro-meteorological conditions. It can accurately predict dynamics in real conditions between two ports, as well as ship turning circles with various rudder angles under calm conditions.

While the preliminary results presented in this chapter are promising, it is important to note that they are limited to specific ship types. Extensive testing is necessary to generalise the suitability of the methods and with the ultimate goal to develop a comprehensive framework for the appropriate utilization of digital twin technology in fleet management.

ACKNOWLEDGMENT

Aalto University authors acknowledge research funding received funding from the Horizons 2020 EU Horizon 2020 project FLARE (Flooding Accident REsponse, Grant No.: 814753-2). All authors asknowedge the financial support received from Horizons Europe project RETROFIT55 (Solutions to achieve 55% GHG reduction by 2030, Grant No.: 101096068). Mingyang Zhang and Spyros Hirdaris express their gratitude for selected sponsorships received from Finnish Maritime Foundation (Merenkulun Säätiö). Special thanks of appreciation go to CSC Finland for the provision of their parallel computing facilities. The views set out in this paper are those of the authors and do not necessarily reflect the views of their sponsors.

REFERENCES

Allen, B. (2021). Digital twins and living models at NASA. In *Digital Twin Summit*. NASA. https://ntrs.nasa.gov/citations/20210023699

Bhattacharya, U., Wu, G., Petrangeli, S., Swaminathan, V., & Manocha, D. (2022). *Show Me What I Like: Detecting User-Specific Video Highlights Using Content-Based Multi-Head Attention.* arXiv preprint arXiv:2207.08352. doi:10.1145/3503161.3547843

Campbell, R., Terziev, M., Tezdogan, T., & Incecik, A. (2022). Computational fluid dynamics predictions of draught and trim variations on ship resistance in confined waters. *Applied Ocean Research*, *126*, 103301. doi:10.1016/j.apor.2022.103301

Chen, Z. S., Lam, J. S. L., & Xiao, Z. (2023). Prediction of harbour vessel fuel consumption based on machine learning approach. *Ocean Engineering*, *278*, 114483. doi:10.1016/j.oceaneng.2023.114483

Coraddu, A., Oneto, L., Baldi, F., & Anguita, D. (2017). Vessels fuel consumption forecast and trim optimisation: A data analytics perspective. *Ocean Engineering*, *130*, 351–370. doi:10.1016/j.oceaneng.2016.11.058

Du, Y., Chen, Y., Li, X., Schönborn, A., & Sun, Z. (2022). Data fusion and machine learning for ship fuel efficiency modeling: Part II–Voyage report data, AIS data and meteorological data. *Communications in Transportation Research*, *2*, 100073. doi:10.1016/j.commtr.2022.100073

Fan, A., Yang, J., Yang, L., Wu, D., & Vladimir, N. (2022). A review of ship fuel consumption models. *Ocean Engineering*, *264*, 112405. doi:10.1016/j.oceaneng.2022.112405

Han, K., Xiao, A., Wu, E., Guo, J., Xu, C., & Wang, Y. (2021). Transformer in transformer. *Advances in Neural Information Processing Systems*, *34*, 15908–15919.

Hasselmann, K., Barnett, T. P., Bouws, E., Carlson, H., Cartwright, D. E., Enke, K., & Walden, H. (1973). *Measurements of wind-wave growth and swell decay during the Joint North Sea Wave Project (JONSWAP)*. Ergaenzungsheft zur Deutschen Hydrographischen Zeitschrift, Reihe A.

Hirdaris, S., & Mikkola, T. K. (Eds.). (2021). *Ship Dynamics for Performance Based Design and Risk Averse Operations*. MDPI.

Holtrop, J., & Mennen, G. G. J. (1982). An approximate power prediction method. *International Shipbuilding Progress*, *29*(335), 166–170. doi:10.3233/ISP-1982-2933501

Hu, Z., Jin, Y., Hu, Q., Sen, S., Zhou, T., & Osman, M. T. (2019). Prediction of fuel consumption for enroute ship based on machine learning. *IEEE Access : Practical Innovations, Open Solutions*, *7*, 119497–119505. doi:10.1109/ACCESS.2019.2933630

Huang, Z., Shen, Y., Li, J., Fey, M., & Brecher, C. (2021). A survey on AI-driven digital twins in industry 4.0: Smart manufacturing and advanced robotics. *Sensors (Basel)*, *21*(19), 6340. doi:10.3390/s21196340 PMID:34640660

ITTC. (2002). *Resistance uncertainty analysis, example for resistance test*. *Proceedings of the 23th International Towing Tank Conference (ITTC), Venice, Italy*.

ITTC. (2014). Analysis of speed/power trial data. *Recommended procedures and guidelines*. ITTC.

ITTC. (2017). *Seakeeping experiments. Recommended procedures and guidelines.* ITTC.

Kaur, M. J., Mishra, V. P., & Maheshwari, P. (2020). The convergence of digital twin, IoT, and machine learning: transforming data into action. *Digital twin technologies and smart cities*, 3-17.

Khan, S., Naseer, M., Hayat, M., Zamir, S. W., Khan, F. S., & Shah, M. (2021). *Transformers in vision: A survey*. ACM Computing Surveys (CSUR).

Kim, Y. R., Jung, M., & Park, J. B. (2021). Development of a fuel consumption prediction model based on machine learning using ship in-service data. *Journal of Marine Science and Engineering*, *9*(2), 137. doi:10.3390/jmse9020137

Kim, Y. R., Steen, S., Kramel, D., Muri, H., & Strømman, A. H. (2023). Modelling of ship resistance and power consumption for the global fleet: The MariTEAM model. *Ocean Engineering*, *281*, 114758. doi:10.1016/j.oceaneng.2023.114758

Lang, X. (2023). *Data-driven ship performance models--emphasis on energy efficiency and fatigue safety* [Doctoral dissertation, Chalmers Tekniska Hogskola (Sweden)].

Lee, J. H., Nam, Y. S., Kim, Y., Liu, Y., Lee, J., & Yang, H. (2022). Real-time digital twin for ship operation in waves. *Ocean Engineering*, *266*, 112867. doi:10.1016/j.oceaneng.2022.112867

Li, N., Liu, S., Liu, Y., Zhao, S., & Liu, M. (2019). Neural speech synthesis with transformer network. *Proceedings of the AAAI Conference on Artificial Intelligence*, *33*(1), 6706–6713. doi:10.1609/aaai.v33i01.33016706

Liu, S., & Papanikolaou, A. (2020). Regression analysis of experimental data for added resistance in waves of arbitrary heading and development of a semi- empirical formula. *Ocean Engineering*, *206*, 206. doi:10.1016/j.oceaneng.2020.107357

Liu, S., Shang, B., Papanikolaou, A., & Bolbot, V. (2016). Improved formula for estimating added resistance of ships in engineering applications. *Journal of Marine Science and Application*, *15*(4), 442–451. doi:10.1007/s11804-016-1377-3

Lou, J., Wang, H., Wang, J., Cai, Q., & Yi, H. (2022). Deep learning method for 3-DOF motion prediction of unmanned surface vehicles based on real sea maneuverability test. *Ocean Engineering*, *250*, 111015. doi:10.1016/j.oceaneng.2022.111015

Luo, S., Ma, N., & Hirakawa, Y. (2016). Evaluation of resistance increase and speed loss of a ship in wind and waves. *Journal of Ocean Engineering and Science*, *1*(3), 212–218. doi:10.1016/j.joes.2016.04.001

Ma, J., Xia, D., Wang, Y., Niu, X., Jiang, S., Liu, Z., & Guo, H. (2022). A comprehensive comparison among metaheuristics (MHs) for geohazard modeling using machine learning: Insights from a case study of landslide displacement prediction. *Engineering Applications of Artificial Intelligence*, *114*, 105150. doi:10.1016/j.engappai.2022.105150

Major, P. Y., Li, G., Zhang, H., & Hildre, H. P. (2021). Real-time digital twin of research vessel for remote monitoring. *Proceedings of 35th European Council for Modelling and Simulation*. IEEE.

Molland, A. F., Turnock, S. R., & Hudson, D. A. (2017). *Ship resistance and propulsion*. Cambridge university press. doi:10.1017/9781316494196

Nielsen, R. E., Papageorgiou, D., Nalpantidis, L., Jensen, B. T., & Blanke, M. (2022). Machine learning enhancement of manoeuvring prediction for ship Digital Twin using full-scale recordings. *Ocean Engineering*, *257*, 111579. doi:10.1016/j.oceaneng.2022.111579

Ouyang, Z. L., & Zou, Z. J. (2021). Nonparametric modeling of ship maneuvering motion based on Gaussian process regression optimised by genetic algorithm. *Ocean Engineering*, *238*, 109699. doi:10.1016/j.oceaneng.2021.109699

Schirmann, M., Collette, M., & Gose, J. (2018). Ship motion and fatigue damage estimation via a digital twin. In *Life Cycle Analysis and Assessment in Civil Engineering: Towards an Integrated Vision* (pp. 2075–2082). CRC Press.

Silva, K. M., & Maki, K. J. (2022). Data-Driven system identification of 6-DoF ship motion in waves with neural networks. *Applied Ocean Research*, *125*, 103222. doi:10.1016/j.apor.2022.103222

Sivaraj, S., Rajendran, S., & Prasad, L. P. (2022). Data driven control based on Deep Q-Network algorithm for heading control and path following of a ship in calm water and waves. *Ocean Engineering*, *259*, 111802. doi:10.1016/j.oceaneng.2022.111802

Staudemeyer, R. C., & Morris, E. R. (2019). *Understanding LSTM—a tutorial into long short-term memory recurrent neural networks*. arXiv preprint arXiv:1909.09586.

Taimuri, G., Matusiak, J., Mikkola, T., Kujala, P., & Hirdaris, S. (2020). A 6-DoF maneuvering model for the rapid estimation of hydrodynamic actions in deep and shallow waters. *Ocean Engineering*, *218*, 108103. doi:10.1016/j.oceaneng.2020.108103

Tillig, F., & Ringsberg, J. W. (2019). A 4 DOF simulation model developed for fuel consumption prediction of ships at sea. *Ships and Offshore Structures, 14*(sup1), 112-120.

UNCTAD. (2022). *Review of Maritime Transport 2022.* UNCTAD.

UNFCCC. (2022). *Long-term low-emission development strategies. Synthesis report by the secretariat*. Sharm el-Sheikh Climate Change Conference.

Uyanık, T., Karatuğ, Ç., & Arslanoğlu, Y. (2020). Machine learning approach to ship fuel consumption: A case of container vessel. *Transportation Research Part D, Transport and Environment*, *84*, 102389. doi:10.1016/j.trd.2020.102389

Vaswani, A., Shazeer, N., Parmar, N., Uszkoreit, J., Jones, L., Gomez, A. N., ... Polosukhin, I. (2017). Attention is all you need. *Advances in Neural Information Processing Systems*, 30.

Vitali, N., Prpić-Oršić, J., & Soares, C. G. (2020). Coupling voyage and weather data to estimate speed loss of container ships in realistic conditions. *Ocean Engineering*, *210*, 106758. doi:10.1016/j.oceaneng.2019.106758

Wang, H. (2020). *Development of voyage optimization algorithms for sustainable shipping and their impact to ship design*. [Doctoral dissertation, Chalmers Tekniska Hogskola (Sweden)].

Wang, Z., Zou, Z., & Soares, C. G. (2019). Identification of ship manoeuvring motion based on nu-support vector machine. *Ocean Engineering*, *183*, 270–281. doi:10.1016/j.oceaneng.2019.04.085

Woo, J., Yu, C., & Kim, N. (2019). Deep reinforcement learning-based controller for path following of an unmanned surface vehicle. *Ocean Engineering*, *183*, 155–166. doi:10.1016/j.oceaneng.2019.04.099

Yan, R., Wang, S., & Psaraftis, H. N. (2021). Data analytics for fuel consumption management in maritime transportation: Status and perspectives. *Transportation Research Part E, Logistics and Transportation Review*, *155*, 102489. doi:10.1016/j.tre.2021.102489

Zeng, D., Xia, G., & Cai, C. (2021, October). Parameter Identification of Hydrodynamic Model of Ship Using EKF. In *2021 China Automation Congress (CAC)* (pp. 1427-1432). IEEE. 10.1109/CAC53003.2021.9727732

Zhang, M., Conti, F., Le Sourne, H., Vassalos, D., Kujala, P., Lindroth, D., & Hirdaris, S. (2021). A method for the direct assessment of ship collision damage and flooding risk in real conditions. *Ocean Engineering*, *237*, 109605. doi:10.1016/j.oceaneng.2021.109605

Zhang, M., Hirdaris, S., & Tsoulakos, N. (2023). A ship digital twin for safe and sustainable ship operations. Build-IT 2023 workshop, Rome, Italy.

Zhang, M., Taimuri, G., Zhang, J., & Hirdaris, S. (2023). A deep learning method for the prediction of 6-DoF ship motions in real conditions. Proceedings of the Institution of Mechanical Engineers, Part M. *Journal of Engineering for the Maritime Environment*. 14750902231157852.

Zhang, M., Tsoulakos, N., Kujala, P., & Hirdaris, S. (2023). A deep learning method for the prediction of ship fuel consumption in real operational conditions. *Engineering Applications of Artificial Intelligence*.